*J. Fluid Mech.* (1980), *vol.* 96, *part* 1, *pp.* 47–64
*Printed in Great Britain*



# On the formation of nonlinear internal waves from the gravitational collapse of mixed regions in two and three dimensions

By T. MAXWORTHY

Departments of Mechanical and Aerospace Engineering,
University of Southern California, Los Angeles, California 90007†

(Received 22 August 1978 and in revised form 26 April 1979)

We show how trains of nonlinear, dispersive waves‡ can be produced by allowing a region of mixed fluid, with a potential energy greater than its surroundings, to collapse towards its equilibrium state. The number of waves and their amplitude depend on the properties of the mixed region and of the ambient stratification. Three different geometrical configurations have been chosen and while each gives qualitatively the same results the form taken by the generated waves and the final equilibrium shape of the mixed region depend critically on these geometrical factors. We relate the internal waves produced by this mechanism to waves produced in natural systems and show that our observations support at least one possible explanation for those found in the oceans and planetary atmospheres.

## 1. Introduction

In many natural systems one of the central questions concerns the character of the flow created when a region of turbulently mixed fluid, with an excess of potential energy, attempts to reach an equilibrium state in a stratified ambient. For example, it now appears that such a mechanism is partially responsible for the appearance of internal waves generated by tidal flow over submarine topography (Halpern 1971; Lee & Beardsley 1974; Gargett 1976; Smith & Farmer 1977; Maxworthy 1978, 1979; to mention a few). It has also been considered as a possible source for features in planetary atmospheres (Maxworthy, Redekopp & Weidman 1978), in the nocturnal inversion (Christy, Muirhead & Hales 1978*a*, *b*), and those generated from thunderstorm downdraughts, Katabatic winds, sea breeze fronts, the spreading of Liquid Natural Gas spills etc. On a basic level the problem has accumulated a substantial number of theoretical efforts (see Mei 1969; Wessel 1969; Padmanabhan *et al.* 1970; Hartman & Lewis 1972; Bell & Dugan 1974; Manins 1976; Kao 1976) based on a rather limited number of experimental findings (Schooley & Stewart 1963; Wu 1969; Schooley & Hughes 1972). For simplicity all of these authors assume the ambient

† Also Jet Propulsion Laboratory, Pasadena, California and the Australian National University, Canberra, Australia.

‡ In some of the cases to be described these are in fact sequences of solitary waves which are ordered by amplitude and which separate in space, as they propagate. In other cases the wave amplitude decreases as the wave propagates, but since the essential balance is between nonlinear steepening and frequency dispersion we feel justified in using the adjective 'solitary' to describe them though they violate the classical description of such waves.

0022-1120/80/4341-8040 $02.00 

density distribution to be linear with height, a condition which is only an approximation to the prototype. The results of Wu (1969) in particular have suggested the existence of three different flow regimes which blend smoothly into one another as time progresses. Of special interest is the so-called 'principal stage' in which the leading edge of the slug moves so that its length increases approximately as $t^{\frac{1}{2}}$. This result has generated a number of papers (e.g. Manins 1976; Kao 1976) that justify the result on theoretical grounds. In a study closely related to the present one (Amen & Maxworthy 1980) we have found that Wu's result is not generally true and that for a large number, but not all cases, the slug length increases more rapidly with time than $t^{\frac{1}{2}}$, e.g. the slug velocity approaches an almost constant value. This result can be most readily explained by using the concepts developed in the present paper in which we consider a parameter range for which a constant slug velocity invariably exists for a finite span of time, in the two-dimensional case at least. The relevant parameters are the ratios of the height $H$ and length $L$ of the mixed region to a characteristic height $h$ of the ambient stratification (the appropriate height is that of the tank in Wu's experiments and the thickness of the stratified layer in ours). In the present experiments we consider two cases. In the first the density distribution is that which exists between two deep layers of miscible fluid as in the work of Benjamin (1967), Davis & Acrivos (1967), Hurdis & Pao (1975) and Ono (1975) for example. While in the second the density distribution consists of a heavy miscible layer on the floor of the experimental tank beneath a light constant density layer [as in case (*a*) of Benjamin (1967), figure 1]. Invariably, in both cases, the vertical scale of the density distribution is small (i.e. $L/h$ and $H/h > O(1)$) and the collapse of the mixed region results in the generation of a number of large-amplitude, internal solitary-waves of the type described by Benjamin, Davis & Acrivos and Ono.† Such large-amplitude waves have, in their simplest form, closed internal streamlines which in the present case consist mainly of mixed fluid from the collapsed region. As the wave propagates it carries this mixed fluid along with it at the appropriate wave speed. In our cases some internal mixing, dissipation and geometric dispersion (in the second case) takes place so that the wave amplitude, and hence the size of the closed streamline region, decreases as the wave propagates. As a result mixed fluid is ejected from the rear of the wave to form a tail behind the wave. Eventually the amplitude of the waves becomes so small that no closed-streamlines region can exist, the mixed fluid can no longer be trapped inside the wave, and it is left behind to enter a new spreading regime governed by a different balance of forces.

In Wu's case it now appears that $h/H$ was so large that only weak solitary waves were formed and the trapping of the mixed region took place for only a short time, if at all. One can actually see the leading solitary wave in his published photographs but the drainage of mixed fluid is so rapid that a constant velocity state is never reached. The cases considered in Amen & Maxworthy (1980), are intermediate between the two extremes and show a mixture of the two effects.

In the second set of experiments reported here we extend the previous work on the two-dimensional case, considered by all authors to date, to three dimensions by allowing the solitary wave to evolve as a cylindrical front with an ever increasing length, measured perpendicular to its direction of propagation. This case approaches the conditions observed in satellite pictures of internal wave signatures revealed by

† Which we call BDO waves in what follows.

their modulation of the surface wave field (e.g. Apel *et al.* 1975) and our results appear to have significance in the interpretation of such images (e.g. Maxworthy 1978).

In all of these cases one is reminded of the similar problem of solitary wave generation in a layer of shallow water with a free surface. In this case if a region of fluid with excess potential energy is released, solitary waves are formed and the whole problem can be analysed using the powerful 'inverse-scattering' method [see Whitham (1974) for example, together with the experimental verification of Hammack & Segur (1974)]. We see that such effects also exist in the present cases and that there must be a strong relationship between all of these results.

## 2. Apparatus and experimental procedures

### 2.1. *Experiments on two-dimensional waves*

As shown in figure 1 the apparatus in this case consists of a 820 cm long, 20 cm wide tank filled with fluid to a total depth of 30 cm. The two layer fluid system was prepared by mixing salt into the bottom layer until a desired density was reached, typically 1·05 g cm$^{-3}$, and then carefully adding fresh water to create a thin layer of density variation in between. By waiting long enough layer thicknesses up to 3 cm could be produced with error function distributions of density within them. Profile shapes (figure 2) were measured using a conventional conductivity probe and demodulation circuit (Maxworthy & Browand 1975). This density distribution was assumed to be of the form $\rho = \bar{\rho}(1 - \bar{\omega}\tanh\alpha y)$ (Benjamin 1967), where $\bar{\rho} = \frac{1}{2}(\rho_1 + \rho_2)$, $\bar{\omega} = (\rho_1 - \rho_2)/(\rho_1 + \rho_2)$, $\rho_1$ and $\rho_2$ are the densities of the two layers and $\alpha^{-1}$ ($\equiv \frac{1}{2}h$) is a characteristic length scale of the density distribution. A barrier could be inserted into grooves at one end of the tank and a *mixed region produced mechanically with a density distribution as shown also in* figure 2.† The barrier could be inserted at various axial locations in order to vary the length of mixed fluid. After all motion due to the mixing had died down the barrier was carefully removed and the flow was observed by photographing both the dyed region and the displacement of either layers of dyed fluid or small neutrally buoyant droplets of carbon-tetrachloride and mineral oil dyed with 'Oil Red O'.

The presence of solitary waves (and their shape) was also indicated by the calibrated conductivity probe which was placed at an appropriate distance downstream of the barrier with its tip at approximately the $\alpha^{-\frac{1}{2}}$ position. This method gave the best indication of the number of waves present and their shape.

### 2.2. *Experiments on three-dimensional waves*

Two sets of experiments were performed *in a tank of square plan form, 245 cm on a side (figures 3a, b). The tank was filled to varying depths, up to 10 cm, with fresh* water. Then 3 litres of very dense, dyed salt solution, with a density of 1·15 g cm$^{-3}$, was introduced at a corner and allowed to spread, initially as a 'gravity current', beneath the fresh water. After about one hour a density distribution of the type

† We also attempted to introduce a region of constant intermediate density ($\bar{\rho}$) but the density profile thus formed did not lend itself to a simple definition of its characteristic height. We note however that this type of distribution (or in fact any with an excess of potential energy over the ambient, see §3.1) gave rise to the production of solitary waves!

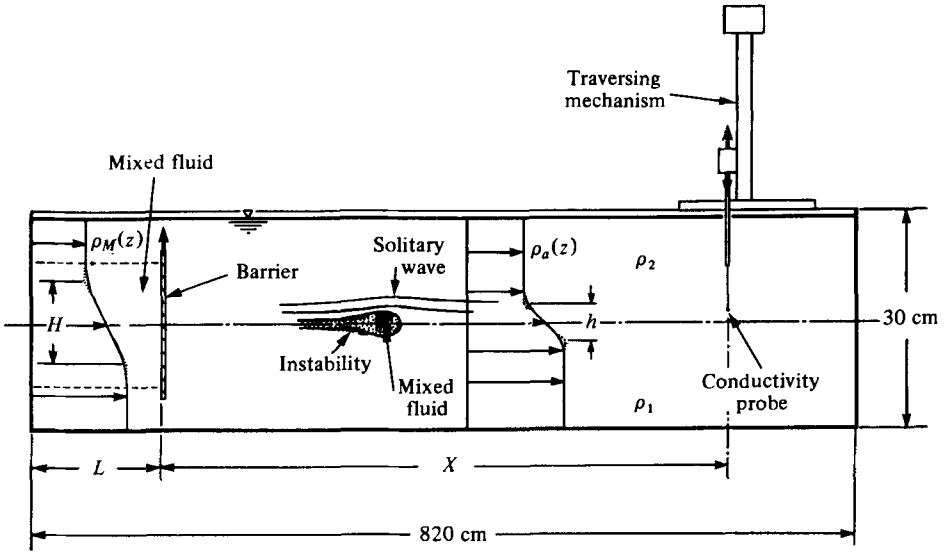


FIGURE 1. Apparatus to study collapse in two dimensions (case 1). Showing definitions of all length scales and form of the initial solitary waves.

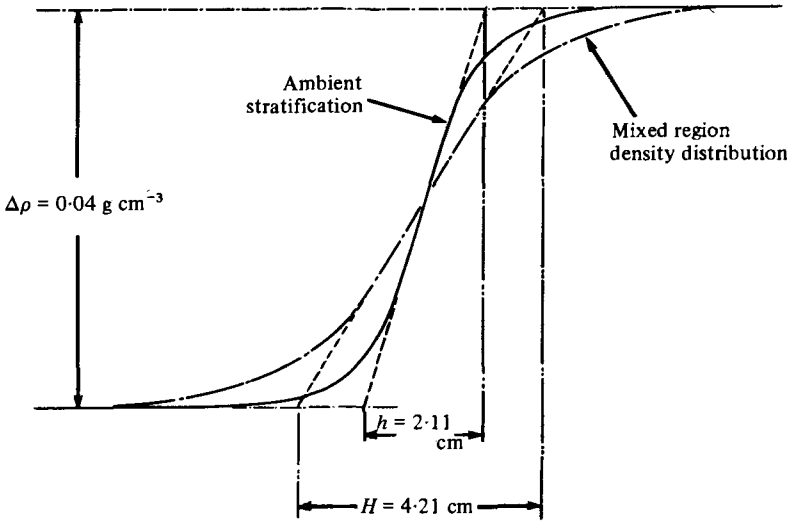


FIGURE 2. Density $\rho$ *vs.* height $z$ for both the ambient and mixed region stratification (case 1). Definition of $h$ and $H$.

shown in figure 3(*a*) and as measured using the conductivity probe (e.g. figure 13) existed uniformly throughout the tank.

In the first set a weighted, plastic cylinder 15 cm in diameter was placed in one corner of the tank and filled with heavy fluid, of density, $\rho_c$ with $1{\cdot}05 < \rho_c < 1{\cdot}15$, to the same level as the free surface in the rest of the tank. The experiment was initiated by suddenly raising the cylinder and allowing the heavy fluid to collapse along the bottom of the tank. The resulting motion was photographed from above since the wave crests that were created, by causing a local increase in the thickness of the

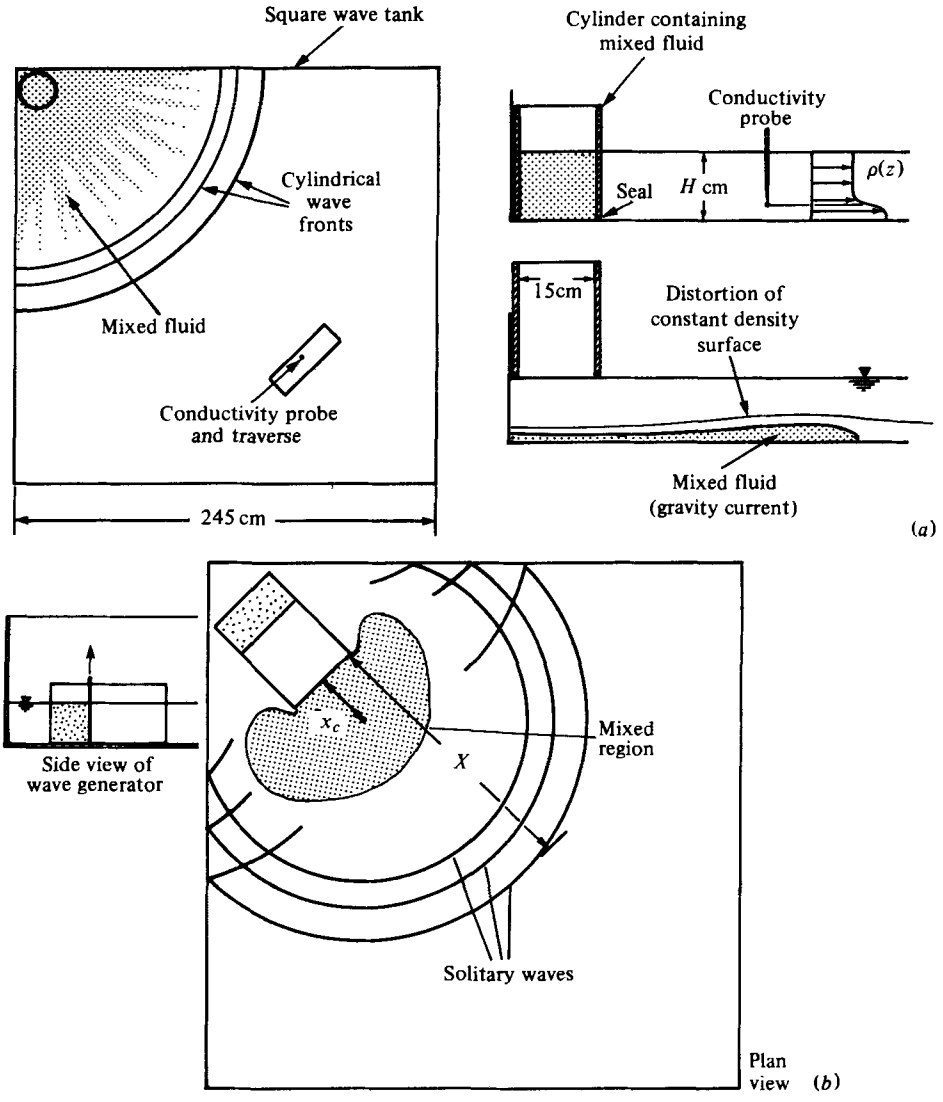


FIGURE 3. (*a*) Apparatus to study the collapse of a mixed region in an axi-symmetric geometry (case 2). Showing method of mixed fluid containment, trapping of gravity current within a cylindrical solitary wave and formation of streaky structure as waves leave the mixed region behind. (*b*) Apparatus to study evolution of a cylindrical wave from an initially plane pulse. Showing generation of a vortex-like mixed region that is eventually left behind by the waves it generates (case 3).

bottom layer, were clearly visible over the majority of their travel. In some cases the mixed fluid was of a different colour from that of the bottom layer in order to clearly distinguish between fluid of these two different origins. The waves were also measured using the conductivity probe placed within the tank with its tip at a pre-determined height and following the density variation at this point as a function of time.

In the second set of experiments the device designed to produce the waves was as shown in figure 3(*b*). It could be operated in several different ways. In one mode

mixed fluid was damned-up in any of the several compartments and when the barrier was removed it was allowed to evolve initially as a plane wave within the box. When it reached the end of the box the mixed region started to spread laterally, as a vortex structure, creating a curved wave as it did so. In the second mode mixed fluid was placed in the rearward compartment and allowed to spread within the total length of the box, i.e. the foremost barrier remained in place. When all wave motion had ceased the front barrier was removed and the mixed region then allowed to evolve. The scheme gave a smaller initial potential energy than the other method and was used to look at the formation of weak waves that were rarely able to carry the mixed fluid very far into the main body of the ambient fluid.

## 3. Results

### 3.1. *Preamble*

We start by noting that almost any form of mixing process within the tanks gave rise to the formation of solitary waves of the BDO type and that they are, in fact, identical to those already described by Davis & Acrivos (1967). For example one could easily produce a solitary wave by simply taking a rod and moving it rapidly back and forth within the interface or pouring in fluid of appropriate density and forming a thermal that spread along the interface (figure 4, plate 1). Such disturbances could not be easily quantified and controlled, however, and the more reproducible methods described in § 2 were used to obtain quantitative results. Of course, in nature it is likely that the mixing processes will not produce clean, well-defined, stationary, mixed regions and this initial comment is necessary to assure the reader that the process to be described still occurs under those less well controlled circumstances. It also gives rise to an interesting corollary which states in its simplest form – that solitary waves are ubiquitous. By which we mean that if a given physical system is capable of supporting solitary wave motions then such motions will invariably arise from quite general excitations.

### 3.2. *Two-dimensional experiments*

In figure 5 (plate 2) we show photographs of the type of solitary waves found in this study. The wave interior contains dye that originated in the mixed fluid behind the barrier and is divided into two elliptically shaped regions placed symmetrically about the centre-line. Thin lines of dye emanate from the rear of these regions and extend back to the origin of the motion. The existence of these dye sheets indicates that this fluid is being continuously ejected from the rear of the wave and that the amplitude of the wave must be decreasing. Further evidence for this decrease is shown in figure 6 where we plot the speed of such a wave *versus* time. The wave speed clearly decreases indicating that the wave amplitude is also decreasing in response to energy dissipation within the wave. Figure 5 also includes an example of the production of a series of such waves and in fact by varying the geometry of the mixed region we have been able to produce up to twelve waves, ordered by amplitude with the largest first, as in figure 5(*a*), for example. In order to put this observation on a firmer footing we have run numerous experiments to determine the dependence of the number of waves on $H/h$ and $L/h$. The results from one such experiment are shown in figure 7 where we plot the output from the conductivity probe as a function of time for the

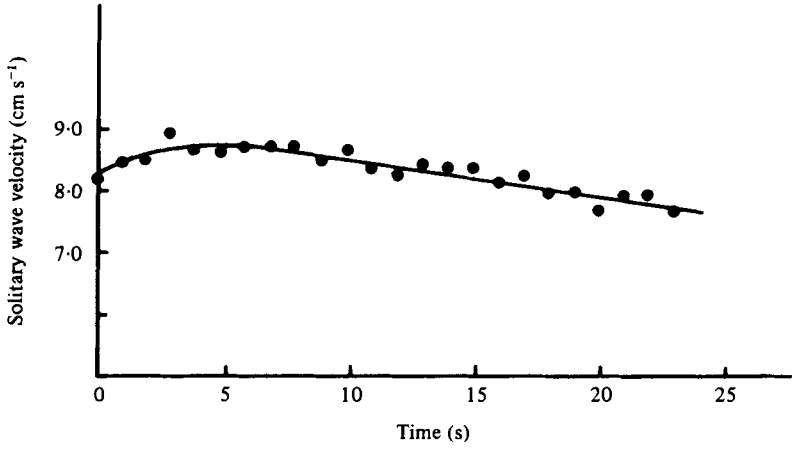


FIGURE 6. Velocity of a two-dimensional wave as a function of time, showing gradual decrease as wave energy is dissipated.

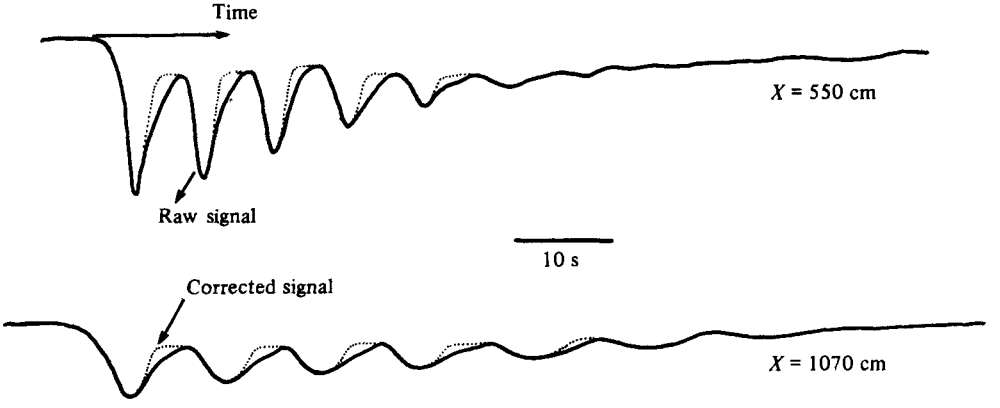


FIGURE 7. Conductivity probe output for designated location and mixed region conditions before ($x$ = 550 cm) and after ($x$ = 1070 cm) reflexion from tank end wall. Showing the evolution of seven solitary waves under these circumstances. $H/h$ = 1·33, $L/h$ = 18·0.

waves as they approach the probe for the first time, at a distance of 550 cm from the origin, and after reflexion from the tank end wall, in which case the equivalent distance is 1070 cm. The existence of seven waves is seen clearly at the latter location. This result and observation of the interaction at the end wall are crucial to our identification of these waves as solitary waves. Firstly, the waves separate as they evolve, they are ordered by amplitude and have a shape appropriate to such a description as already discussed by Davis & Acrivos (1967).† Also their interaction at the end wall is characteristic of solitary waves (Maxworthy 1976), in that the waves suffer a phase delay during the process. Finally in figure 8 we show a composite of all of the results found from a series of such tests. Here we plot the number of waves that evolve ($N$) *versus* $L/h$ and $H/h$. Although the general trends are clear there are some

† We note that although these waves approach the deep water limit of Benjamin (1967) they also contain, theoretically, some aspects of KdV waves (Joseph 1977), and hence the details of BDO theory may not apply exactly. In particular the prediction that there be no solitary wave if the wave volume is too small may be modified by the finite depth of the experimental tank.

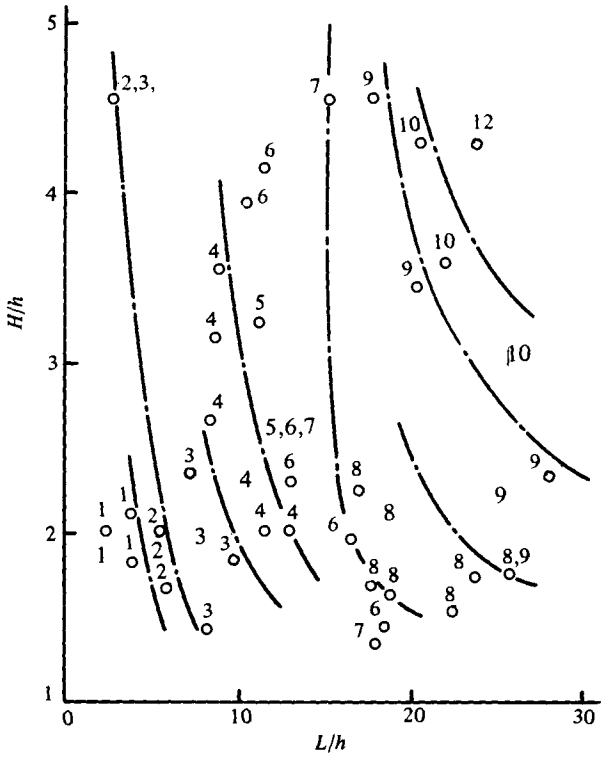


FIGURE 8. Number of waves produced $N$ *versus* extent of mixed region $L/h$ and $H/h$.

ambiguities in such a plot mainly because of our inability to identify the smaller waves from a noisy signal. As a result it is likely that we often missed waves that should have been counted and *vice versa*. Clearly increasing both $L/h$ and $H/h$ increases $N$ with the former parameter being the main control. From limited wave amplitude data it appears that it is $H/h$ that controls this feature but the experiments could not be made precise enough to determine the functional behaviour in a satisfactory manner and so such data are not presented here. We also note that at least one wave is always produced no matter how small the mixed region and this again is typical of some systems that support solitary waves (Whitham 1974).†

### 3.3. *The production of cylindrical solitary waves*

By way of reference, and in order to contrast with the case of collapse in a stratified fluid, we show in figure 9 (plate 3) the generation of a gravity current in an homogeneous fluid. In this case the spread is essentially radial and the leading edge of the mixed region is highly corrugated as in all known plane, two-dimensional experiments (e.g. Simpson 1972). The leading edge continues to propagate but at a slower rate as time progresses and the leading edge corrugations evolve into smaller and smaller scales as it also becomes thinner. Not surprisingly, the dyed, mixed fluid eventually covers the bottom of the tank completely. An $r, t$ diagram showing the evolution of the front is presented in figure 10. In this case the rate of spreading can

† See footnote on previous page.

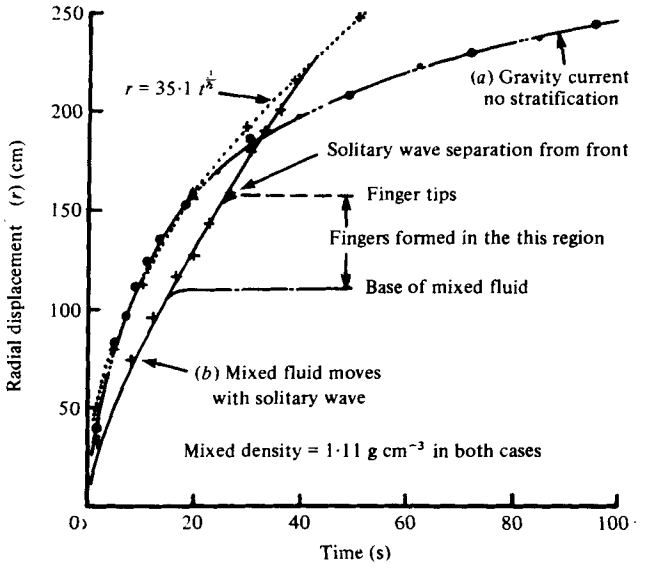


FIGURE 10. (*a*) Radial displacement of leading edge of a gravity current *versus* time in a homogeneous ambient fluid. (*b*) Radial displacement of leading edge and base of mixed region $r$ *versus* time in a stratified ambient fluid. Showing rapid decrease in front velocity once the leading solitary wave separates from the head of the gravity current, and the region in which the fingers or streaks form. The trajectory of the solitary wave is also shown once it has left the mixed region behind.

be described in a quantitative fashion by assuming that the front moves at a critical and constant Froude number [based on the layer depth ($h$)] of order unity in which case $dr/dt \sim h_0^{\frac{1}{2}}$. If we further assume that the volume of fluid is conserved and that the flow is similar then $r^2 h_0 = \text{constant}$. Combining these two results and integrating gives $r \sim t^{\frac{1}{2}}$.† Such a result is also plotted on figure 10 when we have matched the two curves at the triangular point. This result is clearly in reasonable agreement with the experimental findings over the initial portion of the motion but deviates rapidly as, presumably, viscous effects become more important as the layer becomes very thin as in figures 9(*i*, *j*, *k*).

The sequence of events shown in figures 11 and 12 (plates 4–6) shows the essential differences between the effects of a homogeneous and a stratified ambient fluid. In the latter case, initially at least, the front again evolves radially but, as in the two-dimensional case, it is embedded in a large amplitude solitary wave. However, the front is again highly corrugated and is composed of cells of dyed fluid having a width to length ratio of about unity. As the wave evolves and its amplitude decreases this dyed fluid is ejected rearward as long streaks or fingers of dye that terminate when the wave amplitude reaches a critical value for which a recirculation region is no longer possible. The wave continues to propagate while the dye fingers evolve very slowly to a state of equilibrium with the density distribution in their surroundings. This relaxation process involves only an insignificant movement of the dye streaks and they come to rest well before they have spread throughout the tank. In figure 10 we

† I am most grateful to a referee for pointing out to me a result similar to this which, unfortunately, contained a small but significant error.

| $H = 9{\cdot}7$ cm | | |
|---|---|---|
| $\rho_I$ | $N$ | $a$ (mm) |
| 1·015 | 1 | 4·3 |
| 1·029 | 3 | 6·0 |
| 1·053 | 5 | 4·7 |
| 1·065 | 6 | 3·5 |
| 1·078 | 4+ | 8·0 |
| 1·093 | 4+ | 8·3 |
| 1·110 | 6+ | 9·0 |

TABLE 1

also show the evolution of the base and tips of the dye front for this case. In contrast with the previous, homogeneous, case the front velocity is almost constant until a critical wave amplitude is reached and fingers begin to form. We also note the control that is apparently exercised by the ambient stratification in initially, at least, slowing down the gravity current to a velocity smaller than the one it had in the absence of a density distribution (figure 10*a*).

In this case the planform geometry of the mixed region was fixed so that the only available variables for a given ambient stratification were the total height of the fluid layer $H$ and the density $\rho_0$ of the mixed fluid. In table 1 we show how the number $N$ and amplitude† of the waves at a fixed location depends on $\rho_0$ for a given $H$ and $\rho(z)$. As we would anticipate from our previous work the number of waves $N$, at a given location, increases as the density excess and, hence, the potential energy of the mixed region increases. However, the amplitude follows no clear tendency.

In figure 13 we show two of a number of available graphs of the radial displacement of the leading wave as a function of time, together with the ambient density profiles measured in each case and the form of the wave train determined from the conductivity probe located at the indicated positions. Of particular interest is the comparison of the curves for which the zero of time could be determined with reasonable certainty to the trajectory one would expect from simple energy conservation arguments, i.e. $r \sim t^{\frac{2}{3}}$ for small $r$,‡ where we have matched the curves, somewhat arbitrarily, at the triangular points indicated in those figures. Clearly, energy conservation based on a similarity of wave profiles as in Chwang & Wu (1976) for example, is not completely satisfactory and as one possibility we have considered alternative explanations which form the basis of a separate communication (Weidman & Ko 1979). Based on work to be presented in the next section, there is also a suggestion that the differences may be due to our inability to precisely determine the zero of time in these cases. It is also clear that the tank is not large enough for the wave trains to have evolved completely in the more energetic cases (e.g. figure 13*b*) and one is reminded of the similar plots of the wave height in shallow water of Hammack & Segur (1974).

† See legend of figure 13 for the method of determining the amplitudes.

‡ This result comes from assuming a velocity of propagation that varies as $C_0(1+Ka)$ with wave amplitude $a$; using the result of Chwang & Wu (1976) that $a \sim r^{-\frac{1}{2}}$ for energy conservation to hold and then evaluating the resulting integral for small values of $r$ (where $C_0$ is the zero amplitude long-wave speed and $K$ a constant, the values of which depend on the form of the ambient stratification).

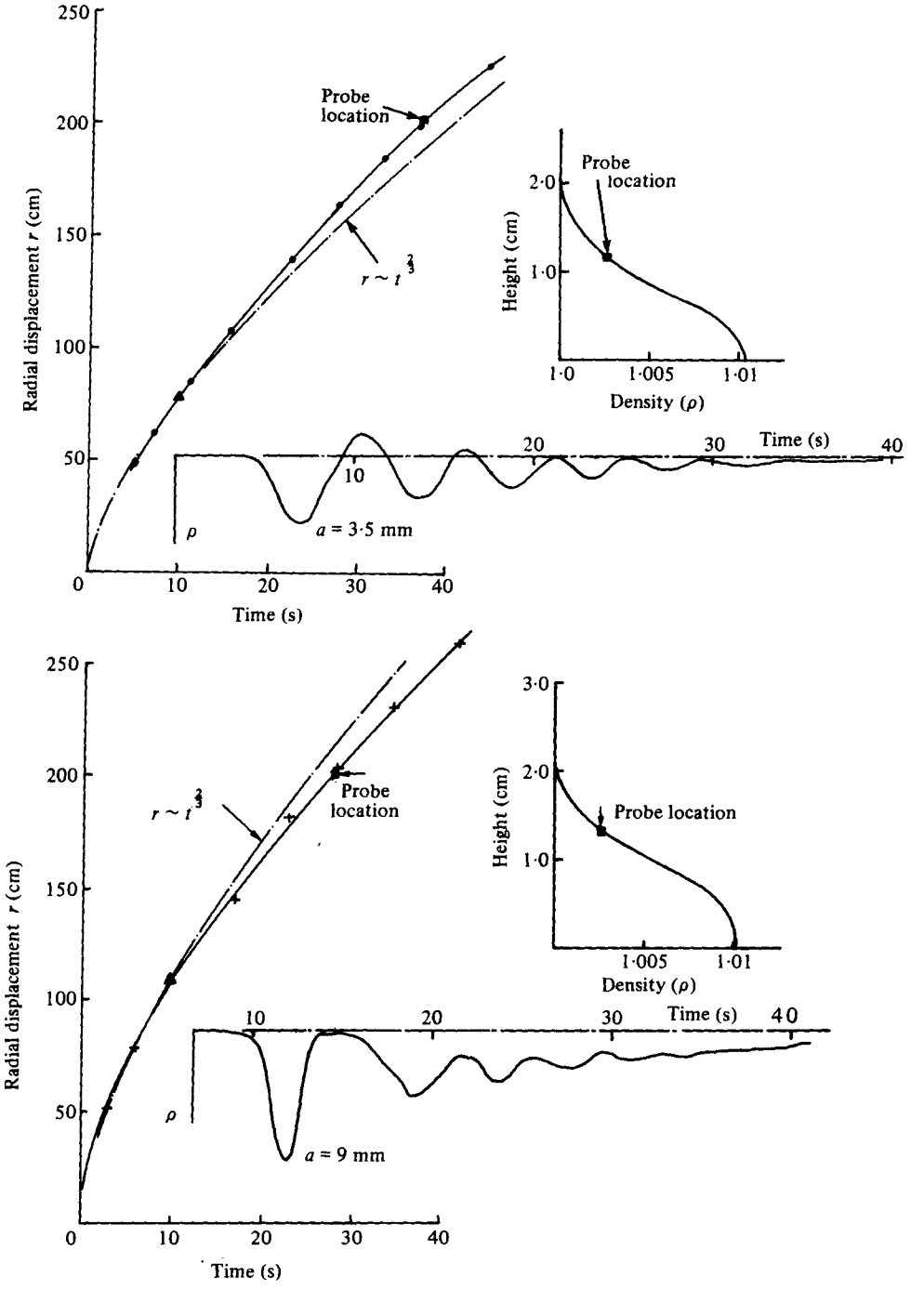


FIGURE 13. (*a*, *b*) In this figure we attempt to show three important characteristics of the evolving cylindrical waves for $H = 9{\cdot}7$ cm. (i) The radial location of the leading cylindrical waves *versus* time. (ii) The density distribution $\rho(z)$ of the ambient fluid before the release of heavier fluid. (iii) The density as a function of time $\rho(t)$ at the location in radius ($r$), the height ($z$) indicated. Scale of $\rho$ is nonlinear in this case. The wave amplitude shown was measured by determining the location of the maximum density under the wave crest on the undisturbed density profile and then subtracting this value of $z$ from the actual location of the probe tip. This method was also used to determine the amplitude values in tables 1 and 2.

The same sequence of photographs (figures 11 and 12) also shows one of the more interesting properties of such two-dimensional waves and is an extension of the work reported in Maxworthy (1976) and Weidman & Maxworthy (1978). We have allowed two cylindrical waves from different sources to interact in such a way that their angle of intersection $\phi$ varies from zero (i.e. a head-on collision, as in Maxworthy 1976) to values approaching 180°. Two observations are particularly interesting. The initial head-on collision approximates that which occurs for two-dimensional plane waves and they suffer a small phase delay, as in the case of shallow-water, free-surface waves (Maxworthy 1976). As the waves continue to propagate the angle between them becomes more obtuse and they cross as a simple X with no apparent change in wave slope at the point of interaction. When this angle reaches a value of approximately 110° a new phenomenon appears. The two vertices forming the X slowly move apart to form two V-shaped regions joined by a new solitary wave of larger amplitude than either of the original waves. In fact under suitable circumstances the new wave has such a large amplitude that it breaks and mixing occurs. As described in Miles (1977*a*, *b*) this is the so-called Mach–stem interaction postulated to occur in shallow water waves obeying the Kadomtsev–Petviashvili (1970) equation. Such a possibility is also discussed in Newell & Redekopp (1977) where it is shown that the Zakharov–Shabat (1974) theory of integrable systems breaks down and that a resonant interaction between solitons can occur. These authors were unable to distinguish between two possible solutions with the relative locations of the nodes in different positions *vis-à-vis* the third soliton. Our experiments have thus shown that it is the type shown in figures 11 and 12 that is likely to be correct in many situations.

Unfortunately the published results of Miles (1977*a*, *b*) cannot be directly applied to the present case so we turn to a case computed recently by Redekopp (private communication) in which he considers two immiscible fluid layers of densities and thicknesses $\rho_1, h_1$ and $\rho_2, h_2$ respectively, with, for convenience, $h_1 < h_2$. In this case the critical value of $\phi$, denoted $\phi_c$, is given by

$$\phi_c = 180° - 2\tan^{-1}\left[\frac{3a}{h_1}\left(1-\frac{h_1}{h_2}\right)\right]^{\frac{1}{2}},$$

where $a$ is the amplitude of the wave of elevation in the thinner layer ($h_1$). He also assumed, as is appropriate for comparison to our experiment that both waves were of the same amplitude. Comparison to even this result is hampered by the fact that both $a$ and $h_1$ have to be estimated from conductivity probe measurements since we have a continuous density variation while the theory assumes a two layer discontinuous density model. For the case shown in figure 11 we use $a \approx 3$ mm, $h_1 \approx 1{\cdot}0$ cm, $h_2 \approx 9$ cm for which case $\phi_c \approx 100°$. Such a result is in reasonable agreement, but, clearly both more theoretical and experimental work needs to be performed before any claim of complete understanding can be made.

### 3.4. *Solitary wave and vortex production in three-dimensions*

In many ways this case is the most interesting and revealing because it gives some feeling for the types of motion that are likely to occur in natural circumstances where a localized disturbance invariably must evolve in three dimensions rather than in the more artificial geometries considered up to now. As an example we quote the results found in Maxworthy (1978) in which the mixed region formed by tidal flow over a

| $\rho_I$ | $N$ | $a$ (mm) |
|---|---|---|
| 1·018 | 2 | 2·4 |
| 1·023 | 3 | — |
| 1·024 | 3 | 2·7 |
| 1·031 | 3 | 4·5 |
| 1·043 | 3 | — |
| 1·060 | 4+ | 5·5 |
| 1·074 | 4+ | — |
| 1·085 | 5+ | — |

TABLE 2

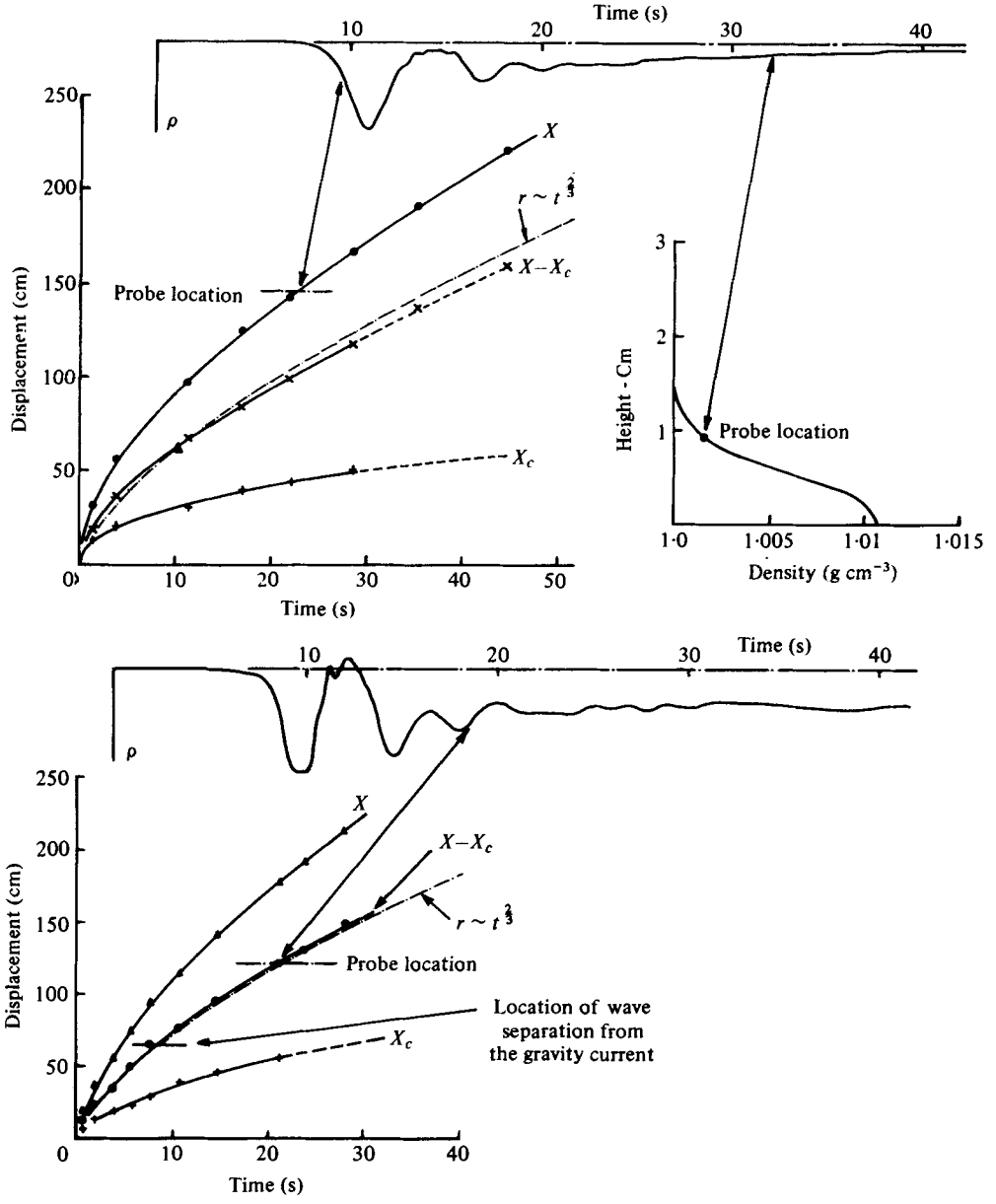


FIGURE 16. (*a*, *b*) $X$, $X_c$ and $X-X_c$ (as defined in figure 3*b*) *versus* time with comparison to $r \sim t^{\frac{2}{3}}$. The density distributions $\rho(z)$ and $\rho(t)$ at the indicated position are also as shown and described in figure 13. $H = 7{\cdot}6$ cm.

ridge evolved into a vortex-like flow that then acted as a 'piston' for the generation of a sequence of solitary waves.

In fact, uch vortex-like structures appear to be a common feature of many satellite observations of the sea surface and appear worthy of concentrated study.

In the present case the initial potential energy excess was produced in a controllable manner as outlined in § 2.2). In figures 14 and 15 (plates 7 and 8) we show photographs of both the vortex and the waves produced in typical cases: (i) where the initial potential energy excess is small and only a weak vortex and waves are formed; (ii) a large initial excess in which case, as before, the leading edge of the vortex is embedded in a wave front and forms a series of fingers (see § 3.2). The number of waves formed also increases as the potential energy of the mixed region is increased (table 2) and they quickly evolve into circular wave fronts from an apparent centre within the final vortex. The details of this evolution are shown in figures 16($a$, $b$), where we plot the distance of the apparent wave centre ($X_c$) and the leading edge of the wave ($X$) (see figure 3$b$) from the mouth of the wave generator. Several points are of interest. (i) The apparent wave centre continues to propagate in a forward direction suggesting that even though the wave appears to be circular in fact the leading edge must be of slightly larger amplitude, and hence wave speed, than the trailing edge and that this makes the whole wave pattern translate slowly in the forward direction. (ii) A measure of the radial rate of spreading ($X - X_c$ *vs.* $t$) is remarkably close to the constant energy curve ($r \sim t^{\frac{2}{3}}$) in this case as opposed to the result of the previous measurements (§ 3.3). The reason for such a difference is not completely clear although one suspects that it may be due to our inability to define the zero of the time absissae with great precision in the latter case. (iii) In both cases the wave shape (i.e. $\rho$ *vs.* $t$) suggests that the waves have not fully evolved and this is in fact reasonable since these two cases represent the one with the largest initial driving potential and, hence, the mixed region and leading wave stay together for a longer time.† (iv) Once the wave has left the mixed fluid behind, the evolution of the latter decreases dramatically and it undergoes only very slow changes as it adjusts to its local surroundings. Presumably both viscous and species diffusion are also important in determining its approach to a final state but this process is so slow that it is of little interest in the present context. It, clearly, has significance in determining the local density distribution (i.e. microstructure) and should be studied further in subsequent experiments.

## 4. Discussion

The results presented in the previous sections are, to a large extent, self-explanatory although it is probably worthwhile listing the major findings compactly. (i) Mixed region collapse in a stratified medium and in both two and three dimensions creates a sequence of solitary waves ordered by amplitude. (ii) In the cases considered here the mixed fluid is invariably trapped within the leading solitary wave and is ejected rearwards as the wave amplitude decreases. When the wave front is long compared to its width this trapping takes place within a number of cells and the ejection process creates a streaky, final distribution of mixed fluid. (iii) Oblique interaction between

† This is in contrast to the water wave case where the motion was produced by an initial raising of the water surface (Hammack & Segur 1974) in which case the wave with the largest driving energy evolved the fastest.

solitary waves can create a resonant condition by which a third larger amplitude wave can be formed between them. (iv) Quite general and uncontrolled mixing events create solitary wave trains and lead us to suspect that they should be excited under many circumstances in natural systems.

We believe the latter observation to be of great importance and now concentrate on a discussion of the role of such a mechanism in nature. In fact, this work was actually motivated by a need to devise a mechanism to generate large-scale, solitary Rossby waves in the Jovian atmosphere (Maxworthy *et al.* 1978). In that case we suggested, based on earlier observations of inertial, solitary wave generation on the cores of vortex rings (Maxworthy 1977), that a zonal shear flow on that planet could become barotropically unstable and generate large-scale vortices which on mixing and collapse would evolve into solitary waves of the correct scale and location to explain certain atmospheric features, notably the Great Red Spot. It now appears that such a mechanism and its extensions can be used to resolve many of the observations of wave motions in natural systems that have been accumulating rapidly over the past several years. Probably the easiest way to classify the different physical circumstances is to consider the various ways in which the mixed region can be produced. The three most obvious are: a shearing instability of some sort (as outlined above); mechanical mixing, by tidal motions for example; convective motions due to vertical and/or horizontal temperature contrasts. To our knowledge only the last two have been explicitly identified as a source of waves. For example, it is now clear that such waves can be created by tidal flow over bottom topograph in the ocean (Halpern 1971; Lee & Beardsley 1974; Gargett 1976; Smith & Farmer 1977; Farmer & Smith 1978; for example). In particular, Gargett (1976) talks of a large pulse of well mixed fluid passing over the crest of a submarine sill on the waning tide. This slug creates solitary waves in much the same way as discussed in this paper and the exact mechanisms have been explored further in Maxworthy (1978, 1979). Another source of mechanically mixed fluid is that in the wakes of submarines travelling through the oceanic thermocline. Such a situation was first modelled by Schooley & Stewart (1963) and Wu (1969), and the ideas of the present paper have been more recently applied to this case by Amen & Maxworthy (1980) who interpreted their results on the collapse of a mixed region in a linearly stratified fluid in terms of solitary wave production.

Examples of solitary waves produced by thermal effects now seem quite common in the meteorological literature and although no analogous observations have been reported in the world's oceans the possibility of such a production mechanism should be anticipated in future measurements. As examples we note that Clarke's (1972) explanation of the 'Morning Glory' phenomenon of North-Central Australia, and the observation on which it is based, has much in common with the present experiments. There the heavy intruding fluid is produced by Katabatic flow from the bordering mountains and although Clarke does not consider this explicitly we believe that such a flow will actually create wave motions in the nocturnal inversion. More recently, Christie *et al.* (1978*a*) have offered, as one interpretation of their observations of solitary waves at Tennant Creek, N.A., the possibility that the waves created by the 'Morning Glory' could propagate as far as their instrument array and produce the observed signals. In a further report (Christie *et al.* 1978) they discuss the generation of waves from gravity currents and our observations coincide in many ways with theirs. Several possibilities exist: (i) the mixed fluid is produced by a shear layer type of

instability that then generates waves in the top layer of the inversion; (ii) Katabatic flow from neighbouring topography does not penetrate to the ground but travels along the top of the nocturnal inversion from the point where the latter intersects the mountain slope; (iii) the waves are generated by the flow and mixing over distant mountains in analogous fashion to the tidal generation mechanism mentioned previously. In other circumstances it appears that the interpretation of the propagation of sea-breeze fronts could well be affected by the considerations of this paper. For example, in Simpson, Mansfield & Milford (1977) the ambient is clearly stratified while the speed of front propagation in the later stages is consistently underestimated by gravity-current theory alone, suggesting control by the speed of long waves on the existing density distribution. Also their description of a 'cut-off' vortex is consistent with our observation of mixed fluid trapped within the leading solitary wave. Other sources are clearly possible under other circumstances, e.g. thunderstorm downdraughts (Goff 1976), wind set-up on inland lakes (Thorpe 1974), squall-lines (Chabra 1972), etc., and we anticipate that many phenomena are likely to be explained in the future by the basic mechanisms put forth in this paper and those referenced above.

The work reported here was performed at U.S.C. under the sponsorship of the Office of Naval Research through Contract no. N000 14-77-C-0015. Casey de Vries built the apparatus and incorporated many ingenious modifications; his help was invaluable. Much of this paper was written during a visit to the Australian National University to which I was most generously invited by Professor J. S. Turner. Many of the figures are the result of the very professional work of Ross Wylde-Browne, while Sandra van der Lee typed the manuscript expertly, and patiently answered my very naïve questions about very essential day-to-day problems that arise when one works in a new, unfamiliar environment.

## REFERENCES

Amen, R. & Maxworthy, T. 1980 The gravitational collapse of a mixed region into a linearly stratified fluid. *J. Fluid Mech.* **96**, 65–80.

Apel, J. R., Byrne, H. M., Proni, J. E. & Charnell, R. L. 1975 Observations of oceanic and internal surface waves from the Earth Resources Technology Satellite. *J. Geophys. Res.* **80**, 865–888.

Bell, T. H. & Dugan, J. P. 1974 Model for mixed region collapse in a stratified fluid. *J. Engng Math.* **8**, 241–248.

Benjamin, T. B. 1967 Internal waves of permanent form in fluids of great depth. *J. Fluid Mech.* **29**, 559–592.

Charba, J. 1972 Gravity current model applied to analysis of squall-line gust-front. NDAA-TM ERL NSSL-61.

Christie, D. R., Muirhead, K. J. & Hales, A. L. 1978*a* Density currents: a source of atmospheric solitons. *Sci. Rep.* R.S.E.S., Australian National University, Canberra.

Christie, D. R., Muirhead, K. J. & Hales, A. L. 1978*b* On solitary waves in the atmosphere. *J. Atmos. Sci.* **35**, 805.

Chwang, A. T. & Wu, T. Y. 1976 Cylindrical solitary waves. *Proc. IUTAM Symp. on Water Waves in Water of Varying Depth.* Canberra, Australia.

Clarke, R. H. 1972 The Morning Glory: An atmospheric hydraulic jump. *J. Appl. Met.* **11**, 304–311.

Davis, R. E. & Acrivos, A. 1967 Solitary internal waves in deep water. *J. Fluid Mech.* **29**, 593–607.

FARMER, D. M. & SMITH, J. D. 1978 Non-linear internal waves in a fjord. In *Hydrodynamics of Estuaries and Fjords* (ed. J. Nihoul). Elsevier.

GARGETT, A. E. 1976 Generation of internal waves in the Strait of Georgia, British Columbia. *Deep Sea Res.* **23**, 17–32.

GOFF, R. C. 1976 Vertical structure of thunderstorm outflow. *Mon. Wea. Rev.* **104**, 1429–1440.

HALPERN, D. 1971 Observations of short period internal waves in Massachusetts Bay. *J. Mar. Res.* **29**, 116–132.

HAMMACK, J. L. & SEGUR, H. 1974 The Korteweg–de Vries equation and water waves. Part 2. Comparison with experiment. *J. Fluid Mech.* **74**, 593–610.

HARTMAN, R. J. & LEWIS, H. W. 1972 Wake collapse in a stratified fluid: Linear treatment. *J. Fluid Mech.* **51**, 613–618.

HURDIS, D. A. & PAO, H.-P. 1975 Experimental observation of internal solitary waves in a stratified fluid. *Phys. Fluids* **18**, 385–386.

JOSEPH, R. I. 1977 Solitary waves in a finite depth fluid. *J. Phys.* (*A : Math. Gen.*) **10**, L255–227.

KADOMTSEV, B. B. & PETVIASHVILI, V. I. 1970 On the stability of solitary waves in weakly dispersive media. *Dokl. Akad. Nauk S.S.S.R.* **15**, 753 (*Sov. Phys. Dokl.* **15**, 539).

KAO, T. W. 1976 Principal stage of wake collapse in a stratified fluid: Two-dimensional theory. *Phys. Fluids* **19**, 1071–1074.

LEE, C. Y. & BEARDSLEY, R. C. 1974 The generation of long non-linear internal waves in a weakly-stratified shear flow. *J. Geophys. Res.* **79**, 453–462.

MANINS, P. C. 1976 Mixed-region collapse in a stratified fluid. *J. Fluid Mech.* **77**, 177–183.

MAXWORTHY, T. 1976 Experiments on collisions between solitary waves. *J. Fluid Mech.* **76**, 177–185.

MAXWORTHY, T. 1977 Some experimental studies of vortex rings. *J. Fluid Mech.* **81**, 465–495.

MAXWORTHY, T. 1978 A mechanism for the generation of internal solitary waves by tidal flow over submarine topography. *Ocean Modelling*, no. 14, Department of Applied Mathematics & Theoretical Physics, University of Cambridge.

MAXWORTHY, T. 1979 A note on the internal solitary waves produced by tidal flow over a three-dimensional ridge. Submitted to *J. Geophys. Res.*

MAXWORTHY, T. & BROWAND, F. K. 1975 Experiments in rotating and stratified flows: Oceanographic application. *Ann. Rev. Fluid Mech.* **7**, 273–305.

MAXWORTHY, T., REDEKOPP, L. G. & WEIDMAN, P. D. 1978 On the production and interaction of planetary solitary waves: Applications to the Jovian atmosphere. *Icarus* **33**, 388–409.

MEI, C. C. 1969 Collapse of a homogeneous fluid mass in a stratified fluid. *Proc. 12th Int. Cong. Appl. Mech.* pp. 321–330. Springer.

MILES, J. W. 1977*a* Obliquely interacting solitary waves. *J. Fluid Mech.* **79**, 157–170.

MILES, J. W. 1977*b* Resonantly interacting solitary waves. *J. Fluid Mech.* **79**, 171–179.

NEWELL, A. C. & REDEKOPP, L. G. 1977 Breakdown of Zakharov–Shabat theory and soliton creation. *Phy. Rev. Lett.* **38**, 377–380.

ONO, H. 1975 Algebraic solitary waves in stratified fluids. *J. Phys. Soc. Japan* **39**, 1082–91.

PADMANABHAN, H., AMES, W. F., KENNEDY, J. F. & HUNG, T-K. 1970 A numerical investigation of wake deformation in density stratified fluids. *J. Engng Math.* **4**, 229–241.

SAWYER, C. & APEL, J. R. 1976 Satellite images of ocean internal-wave signatures. N.O.A.A. S/T2401.

SCHOOLEY, A. H. & STEWART, R. W. 1963 Experiments with a self-propelled body submerged in a fluid with a vertical density gradient. *J. Fluid Mech.* **15**, 83–96.

SCHOOLEY, A. H. & HUGHES, B. A. 1972 An experimental and theoretical study of internal waves generated by the collapse of a two-dimensional mixed region in a density gradient. *J. Fluid Mech.* **51**, 159–175.

SIMPSON, J. E. 1972 Effects of the lower boundary on the head of a gravity current. *J. Fluid Mech.* **53**, 759–768.

SIMPSON, J. E., MANSFIELD, D. A. & MILFORD, J. R. 1977 Inland penetration of sea-breeze fronts. *Quart. J. Roy. Met. Soc.* **103**, 47–76.

SMITH, J. D. & FARMER, D. M. 1977 Non-linear internal waves and internal hydraulic jumps in a fjord. In *Geofluiddynamic Wave Mathematics*, pp. 42–53. University of Washington, Seattle.

THORPE, S. A. 1974 Near resonant forcing in a shallow two-layer fluid: A model for the interna surge in Loch Ness. *J. Fluid Mech.* **63**, 509–527.

WEIDMAN, P. D. & MAXWORTHY, T. 1978 Experiments on strong interactions between solitary waves. *J. Fluid Mech.* **85**, 417–432.

WEIDMAN, P. D. & KO, K. 1979 Weakly non-linear cylindrical gravity waves. To be submitted for publication.

WESSEL, W. R. 1969 Numerical study of the collapse of a perturbation in an infinite density stratified fluid. *Phys. Fluids Suppl.* **12**, II 171–176.

WHITHAM, G. B. 1974 *Linear and Non-Linear Waves*. Wiley.

WU, J. 1969 Mixed region collapse with internal wave generation in a density-stratified medium. *J. Fluid Mech.* **56**, 265–276.

ZAKHAROV, V. E. & SHABAT, A. B. 1974 A scheme for integrating the nonlinear equations of mathematical physics by the method of the inverse scattering problem. *Funct. Anal. & Appl.* **8**, 226–235.

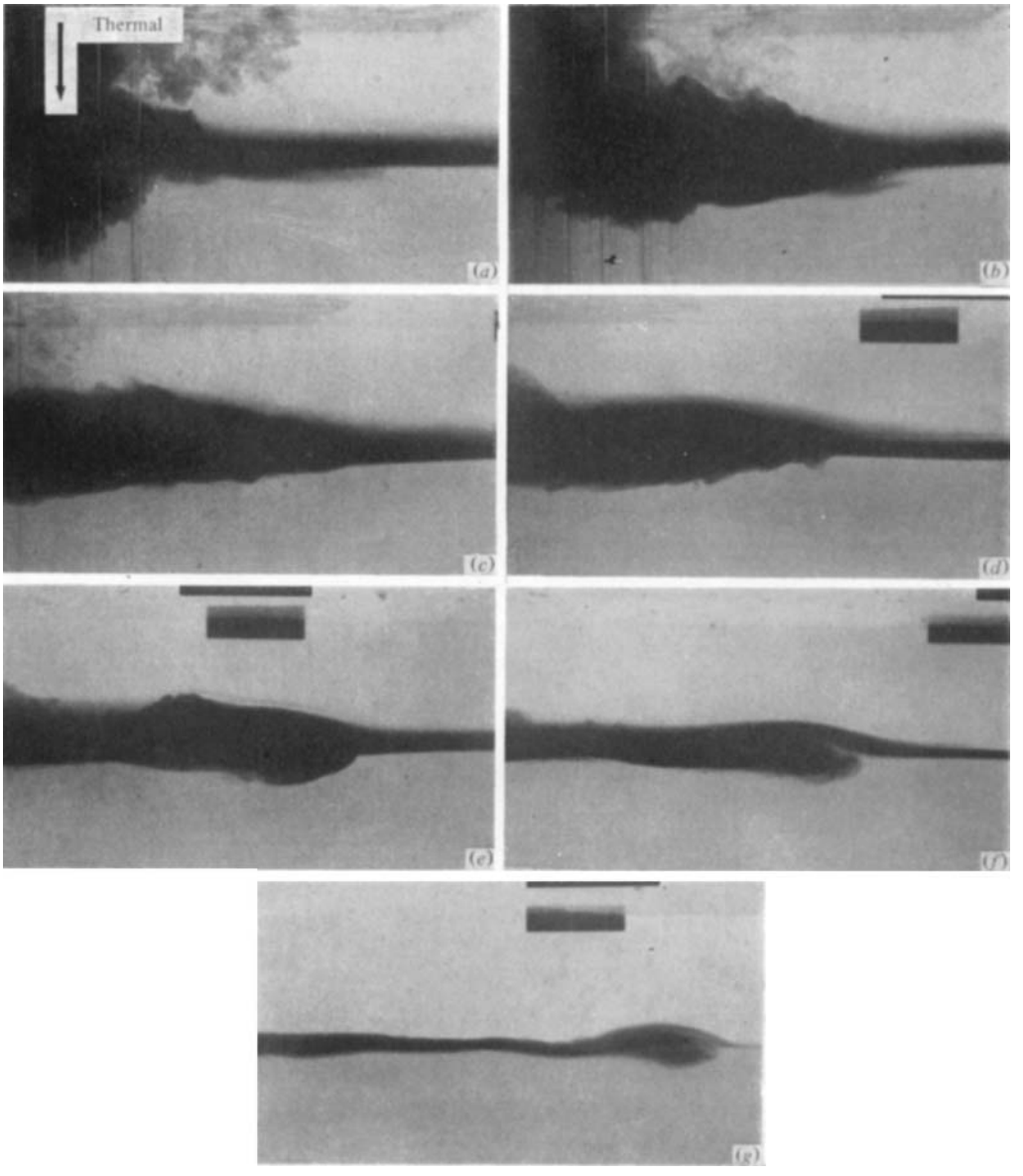


FIGURE 4. Two-dimensional solitary waves produced by impingement of a thermal onto the fluid interface which then evolves along the interface as a series of solitary waves.

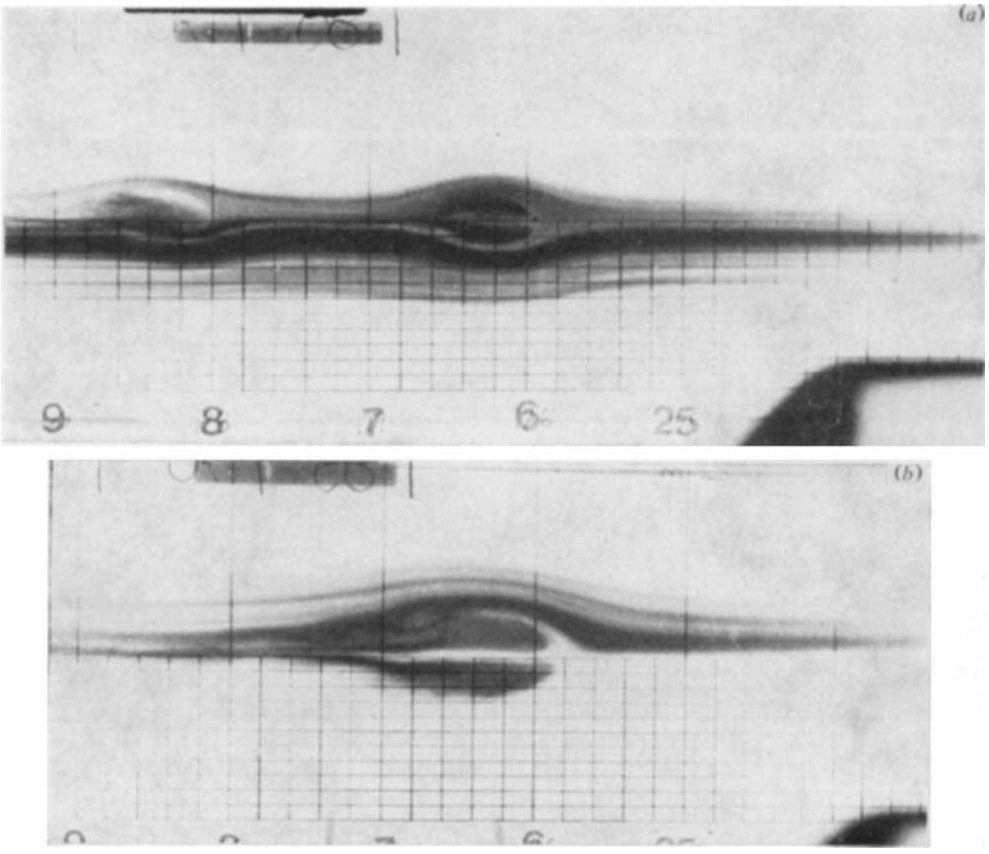


FIGURE 5. (*a*) Photograph of two-dimensional waves of large amplitude that carry along mixed fluid after the collapse. (*b*) The same as (*a*) except that the wave amplitude is so large that a critical Richardson number is attained at the rear of the head and mixing takes place.

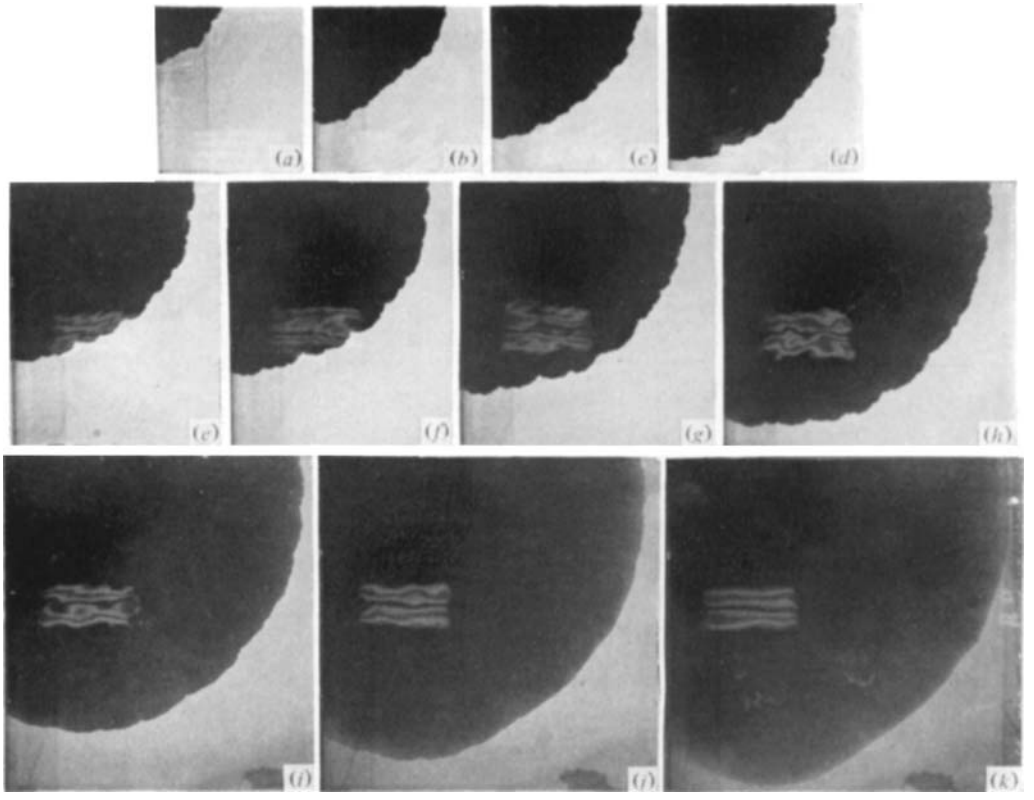


FIGURE 9. Sequence of photographs of a cylindrical gravity current propagating in a homogeneous ambient. Times and locations given by the solid points of figure 10(*a*).

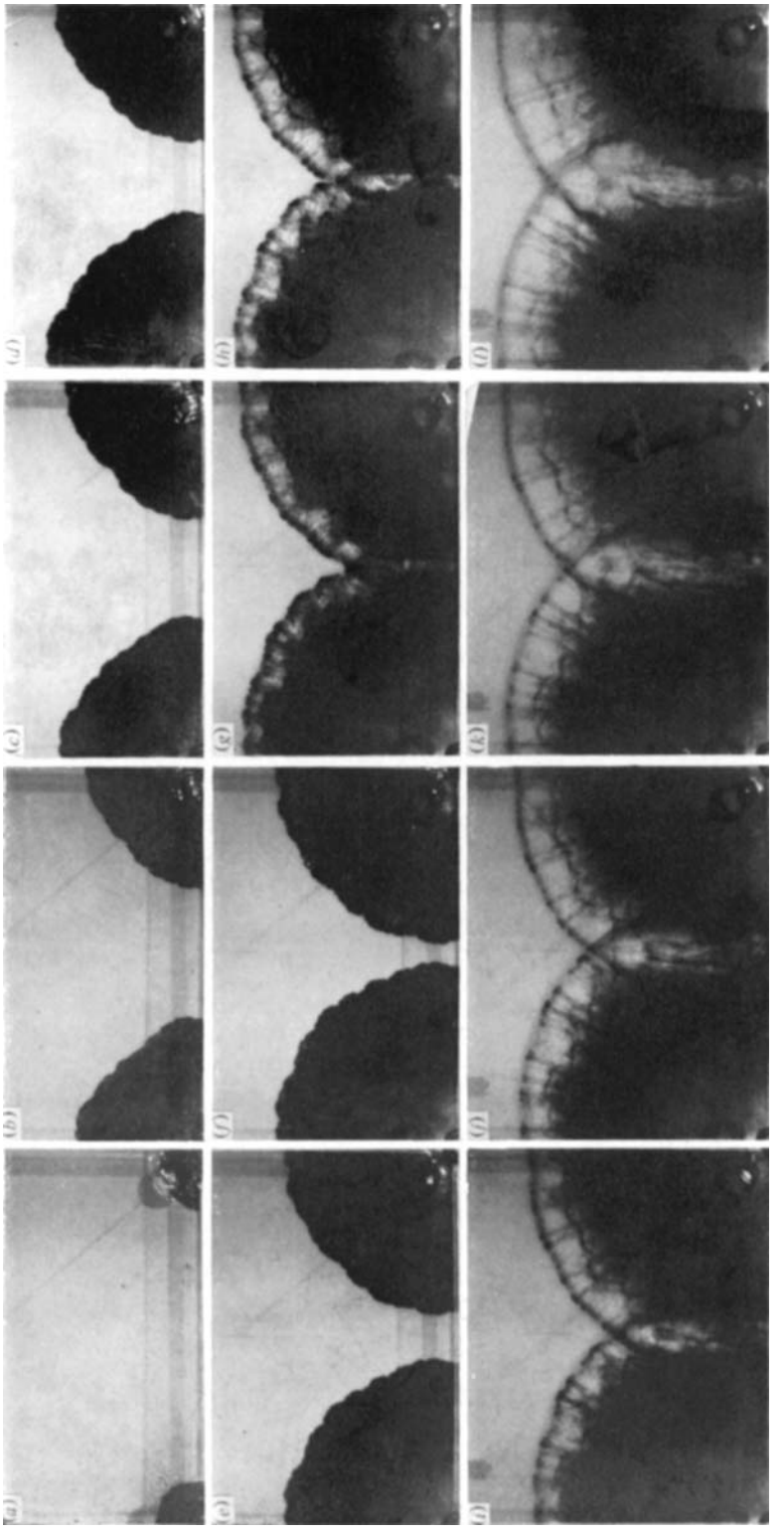

FIGURE 11. For legend see facing page.

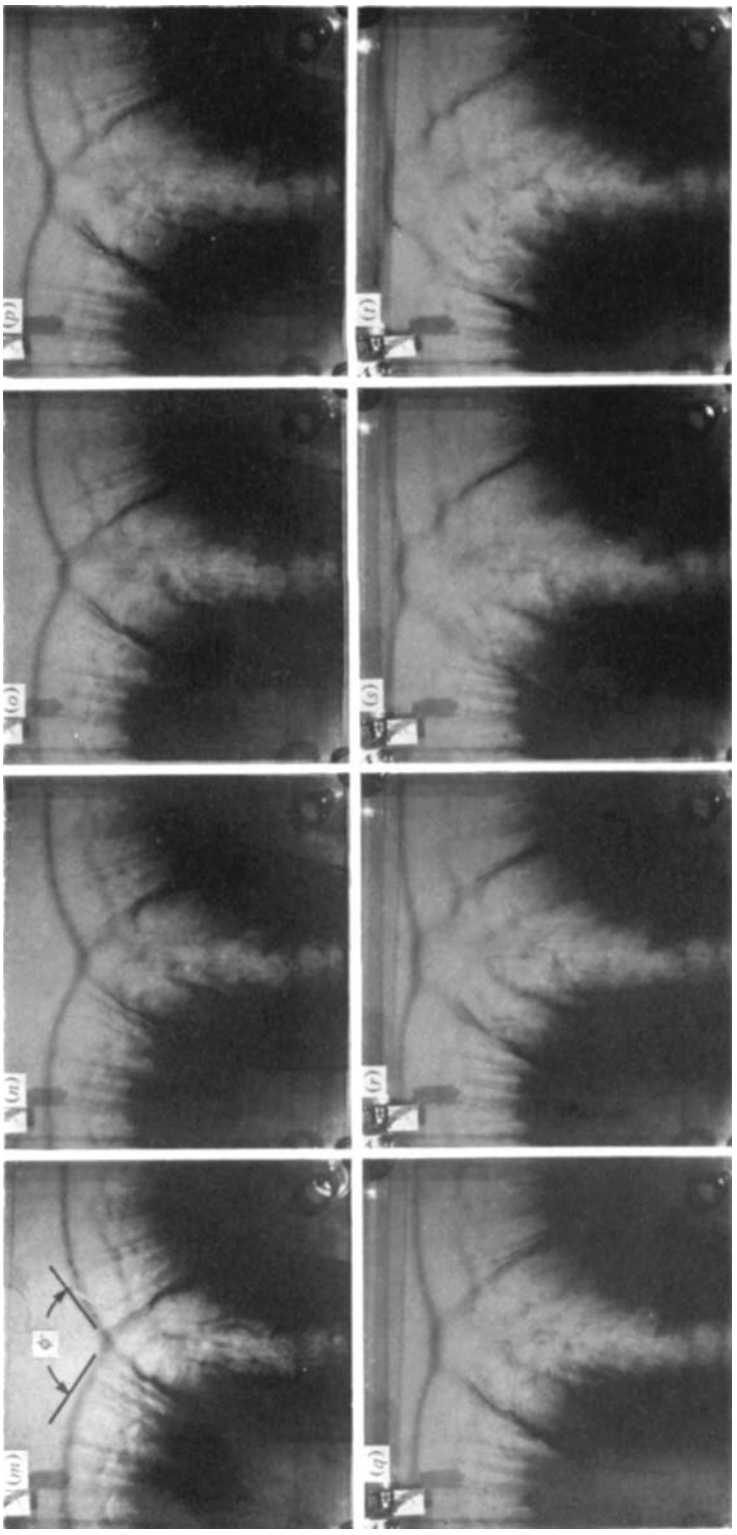


FIGURE 11. Photographic sequence of a gravity current producing solitary waves from sources placed in two corners of the large square tank. Before interaction, the sequence shows how the leading solitary wave traps mixed fluid in a series of cells which slowly deposit this fluid behind the wave. The result is a series of fingers of mixed fluid penetrating into the ambient stratification. The point of intersection of the waves evolves further to produce a third wave between them when a critical crossing angle ($\phi_c$) is reached.

FIGURE 12. Details of the cellular structure embedded in the leading wave. One typical example is indicated by arrows although others can be picked out readily in (*a*)–(*e*). In (*f*) we show details of the top right-hand corner of figure 11(*t*) where further resonant interactions occur between the main wave, from the left, and the following waves, from the right-hand collapse region. Here '1' indicates the main interaction while '2' and '3' are the secondary cases. Compare to Gargett (1976, figure 3) where such multiple interactions can be seen in the surface layers of the Strait of Georgia, B.C. Also see Sawyer & Apel (1976, plate 6) (image of 14 July 1974) for an observation of a single interaction.

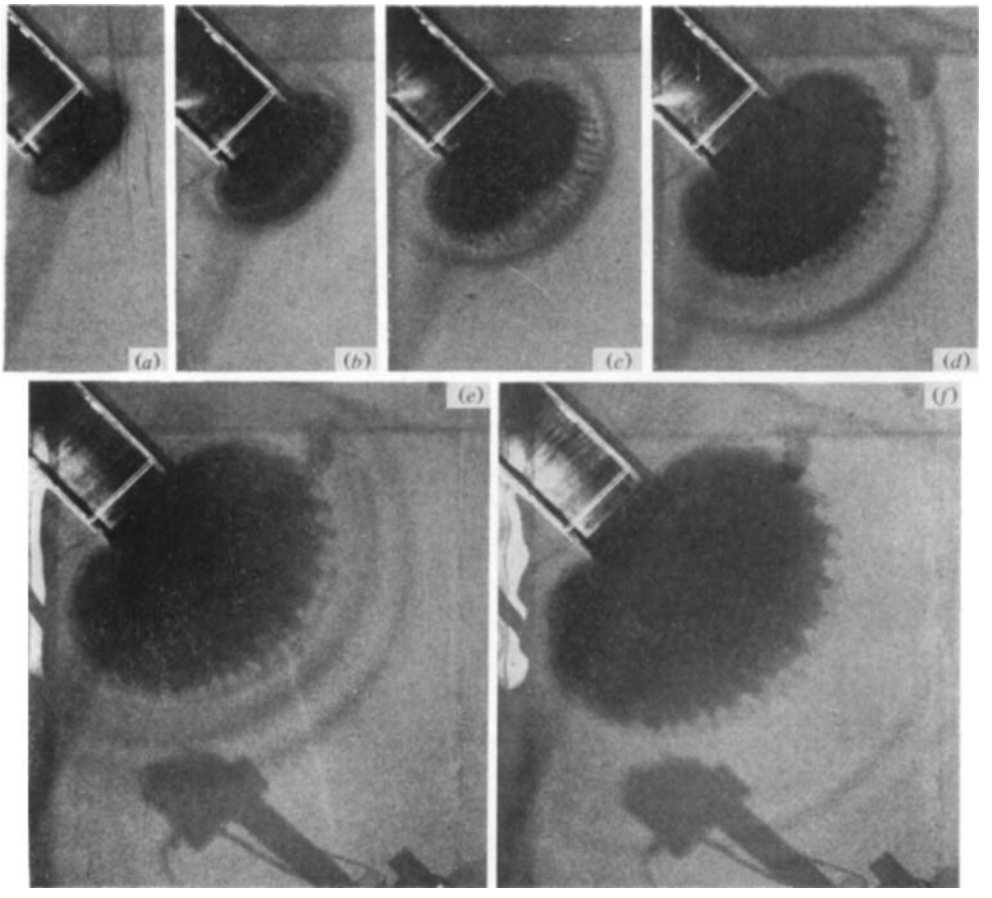


FIGURE 14. Photographic sequence of waves produced by a small initial potential energy difference. Showing rapid separation of waves from the mixed region and its continued development thereafter (case 3).

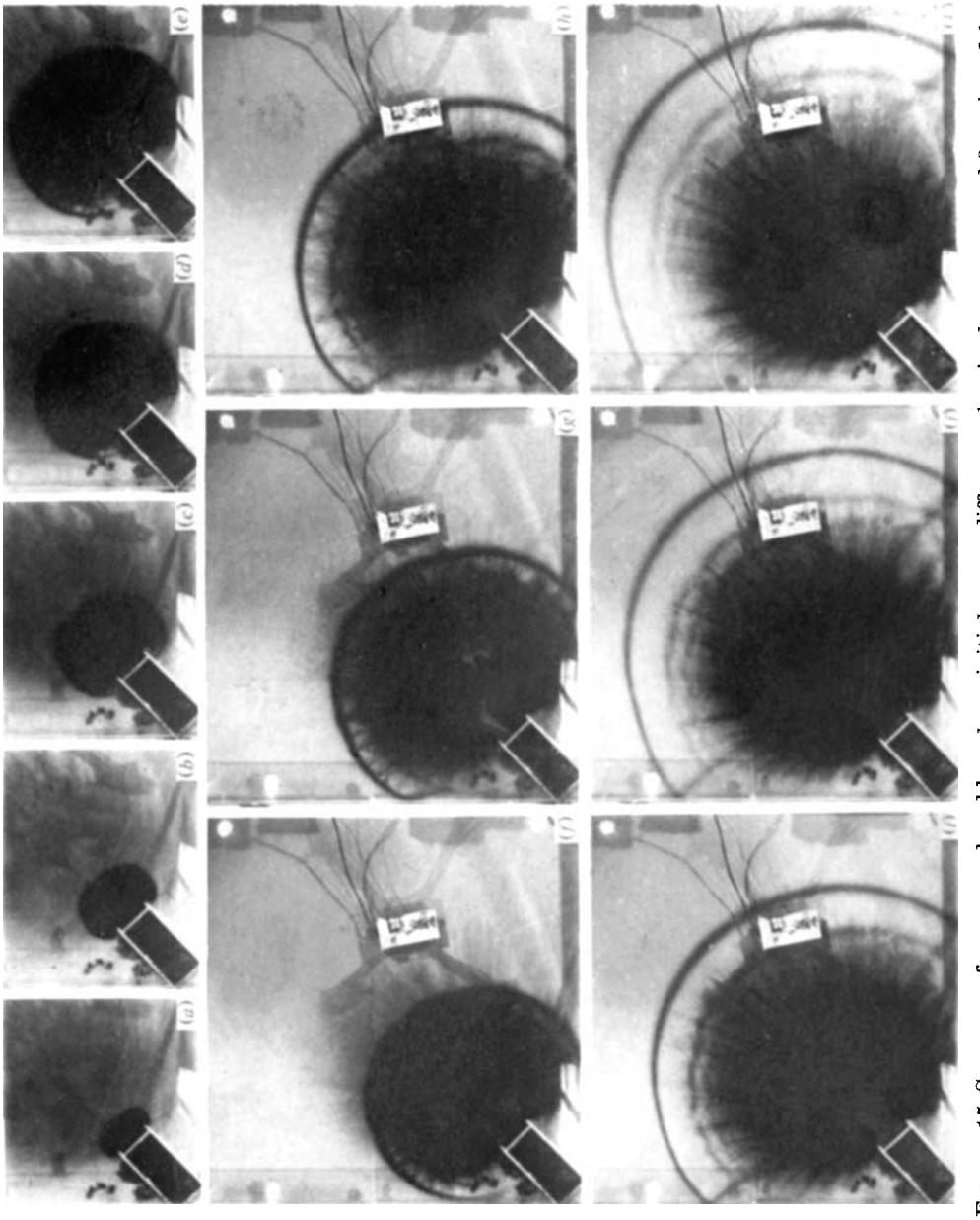

FIGURE 15. Sequence of waves produced by a large initial energy difference showing large waves and fingering of the mixed region (as defined in figure 3*b*). The dark patch with streaks and vortices, in (*a*)–(*g*), is from a previous experiment.